A PARFOCALITY MEASUREMENT METHOD OF A CONTINUOUS ZOOM STEREO MICROSCOPE

Yigang Wang[1,2], Gangyi Jiang[1,*], Mei Yu[1], Feng Shao[1], Wang Yuan[1]

[1] Faculty of Information Science and Engineering

Ningbo University, No.818 Fenghua Road, 315200

Ningbo, China

[2] Dept. of Information, Ningnbo Institute of Technology

Zhejiang University, No.1 Qianhu South Road, 315010

Ningbo, China

[*] Emails: jianggangyi@126.com

Submitted: Dec.30, 2012 ***Accepted: July 3, 2013*** ***Published: Sep. 3, 2013***

Abstract- To satisfy the demands of the continuous zoom stereo microscope, a parfocality measurement method is proposed. First, the mechanical parameters of the focusing system are estimated by testing the highest and the lowest displacements of the lens group and the rotation angle of the knob simultaneously. Second, by analyzing images captured under different zoom rates, the relatively sharpest displacement under a specified zoom rate is obtained according to the values of the four definition functions, including the variance function, the gradient square function, the discrete Fourier transform function and the Walsh-Hadamard transform function. Then, an in-focus model is presented and implemented to determine whether or not the relatively sharpest displacement under a specified zoom rate is an in-focus displacement, and to obtain the discrete in-focus displacements under multi-

rates. Finally, by using discrete in-focus displacements, a continuous zoom in-focus curve is fitted. Results from the experiments show that the proposed method can accurately and effectively measure the parfocality of a continuous zoom stereo microscope.

Index terms*: Continuous zoom, stereo microscope, parfocality, definition function, in-focus model.*

I. INTRODUCTION

Stereo microscopes, which can observe and record a stereo image, are playing more and more important roles in industry[1]. Some specific applications, such as stereo measurement, auto-operation, three dimensional (3D) reconstruction can also be realized [2-3]. Distance estimation is an essential problem in many fields[4-5], especially in the field of stereo micromanipulation. This can enable a robot that is controlled according to high resolution stereo microscope image processing to move accurately [6-8]. Moreover, continuous zoom stereo microscopes are used in a broader range of fields in order to provide sharp images under different zoom rates [9]. Parfocality is a characteristic of a continuous zoom stereo microscope that, if the image obtained with a microscope is adjusted to be sharp under a high zoom rate, the image shall remain sharp while the zoom rate is adjusted from high to low. However, the parfocality of a stereo microscope will decrease if some lenses, which belong to the lens group of a microscope, move away from their initial location as a result of vibrations or other reasons. This often happens when the lens group is transported from a manufacturing plant to an assembly factory. Thus, it is necessary to accurately measure the parfocality of a continuous zoom stereo microscope before assembly. In order to take an accurate measurement, first, find the sharpest image under a special zoom rate by using a focusing system. Then, determine whether or not the sharpest image is an in-focus image, however, due to the limitation of the adjusting range of the focusing system, the sharpest image obtained under a special zoom rate may fail to be sharp when the microscope is out-of-focus.

The definition function is an effective tool to find the relatively sharpest image under a special zoom rate. Generally, the definition of an image can be evaluated in the spatial domain or the frequency domain. There are several spatial-domain-based functions, such as the image entropy function, the high order statistic function, the variance function, and so on. Among them, the variance function is proven to be the most effective [10]. Besides the above mentioned functions,

other functions that are based on edge detection, such as the absolution gradient function, the gradient square function, the Laplacian model function [11], etc., also belong to spatial-domain-based methods with the gradient model being the most effective. Frequency domain functions usually include the discrete Fourier transform (DFT), the discrete cosine transforming (DCT), the discrete wavelet transforming (DWT), the Walsh-Hadamard transforming (WHT)[12-13], and so on. In addition, the definition functions can be applied in many fields. One important application is autofocus, where the improved DCT function or other functions are adopted to carry out robust or quick auto focusing [14-16]. Out-of-focus image retrieval is another field where a phase exit model is established to retrieve an out-of-focus image [17].

By analyzing the definition of images captured under different zoom rates, a multi-rate in-focus model is presented in this paper. Then, based on the model, a new method to measure the parfocality of a continuous zoom stereo microscope is proposed. First, the relatively sharpest image under special zoom rate is found by using the definition function. When the lens group locates at the point where the relatively sharpest image is obtained, the displacement between the lens group and the object stage is defined as the relatively sharpest displacement. Since a rotating knob drives the lens group, the rotating angle of the knob can be used to represent the displacement of the lens group. The corresponding mechanical parameter, which indicates how far the lens group should be moved when knob is rotated with 1°, is computed. Second, the relatively sharpest displacements under each zoom rate are computed. Third, the relatively sharpest displacement can be classified as an in-focus displacement according to the multi-rate in-focus model. Here, the in-focus displacement is the distance from the object stage to the lens group. At the same time, the sharpest image, namely the in-focus image, can be acquired when the lens group locates the in-focus displacement. Finally, the continuous zoom in-focus curve is fitted by the least-squares method based on the discrete in-focus displacement and the mechanical parameter.

II. FIELD DEPTH ESTIMATION OF A MICROSCOPE

Due to the existence of field depth, an in-focus displacement is not unique. When a microscope is focusing on an object plane, the planes in front of the object plane and behind the object plane

can also be sharply placed in focus, and the distance between these two planes is defined as the field depth.

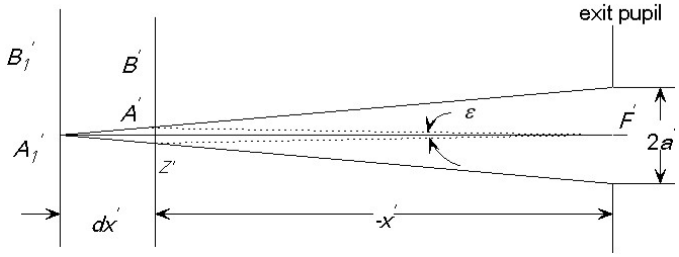

Figure 1. Illustration of field depth

Figure 1. shows the image side of a lens, while the opposite is called the object side. In the figure, $A'B'$ denotes the object-image plane. The original object of $A'B'$ is at the object plane. If there is an object in front of the object plane, the converging rays from this object are projected on the object-image plane after reaching a sharp focus on $A_1'B_1'$, which is on the plane that is in front of the object-image plane [18]. The image on the object-image plane is a small disk called the circle of confusion. Therefore, the projection of point A_1' in the plane $A'B'$ is the circle of confusion. Z' denotes the diameter of the circle. The distance between planes $A'B'$ and $A_1'B_1'$ is denoted as dx'. Since $A'B'$ is an object-image plane, it takes no difference whether the location is at the exit pupil or the focal plane. Given that $2a'$ denotes the diameter of the exit pupil, then the diameter Z' satisfies

$$\frac{Z'}{2a'} = \frac{dx'}{-x' + dx'} \tag{1}$$

Let ε denote the limiting angle of resolution for the eye. If the opening angle, which is from the center of the exit pupil F' to boundary of the circle of confusion, is not more than ε, it is easy to see that the image of the circle of confusion in the brain is only one point, not a circle. Let $2dx'$ denote the depth from the front image plane of the object-image plane to the back image plane, moreover, let the object between the two corresponding planes be sharply imaged. According to the optical path equation, the distance between the two planes on the object side, denoted as $2dx$, can be computed as follows

$$2dx = \frac{250n\varepsilon}{MA} \tag{2}$$

where n is the whole refractive index of the lens group, A is the numerical aperture of the microscope, and M is the zoom rate. Generally, n is set as 1, and ε is set to be 0.00029. The

limiting angle of resolution for eye is equal to 1′. At the same time, the numerical aperture and the corresponding field depth under the different zoom rate used in this paper are shown in table 1. The field depth under the minimal zoom rate is about 30 times larger than that under the maximal zoom rate, and the latter is only approximately 126 μm. In order to obtain the sharpest image, a high-precision adjustment precision is needed.

Table 1. Numerical aperture and estimated field depth

Rate	Numerical Aperture	Field depth (mm)
0.8	0.025	3.625000
1	0.030	2.416667
2	0.052	0.697115
4	0.080	0.226563
5	0.090	0.161111
6.5	0.096	0.125868

III. THE PROPOSED PARFOCALITY MEASUREMENT METHOD

In order to measure parfocality of a stereo microscope, first, the mechanical parameter should be obtained to establish a relationship between the captured image and the displacement of the lens group. Then, following in order from high zoom rates to low zoom rates, several images are taken under each rate and each lens group displacement. By computing the value of the definition function for of images, the relatively sharpest image is obtained under different zoom rates. Third, it is determined whether or not the relatively sharpest image is in-focus. Finally, the continuous zoom in-focus displacement curve is fitted with the least-squares method based on discrete in-focus displacements. The system diagram of the proposed method is shown in figure 2.

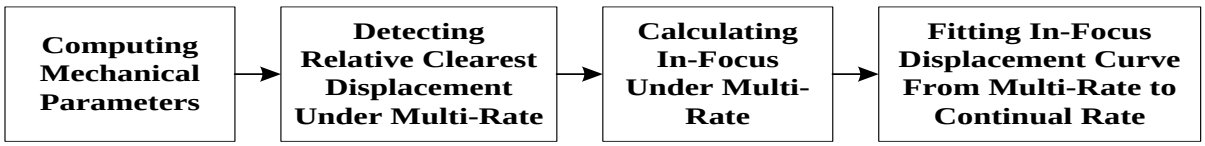

Figure 2. Block diagram of the proposed parfocality measurement method for a continuous zoom stereo microscope

a. Computing the proportion of the rotating angle of knob to the lens group displacement

The lens group of the stereo microscope can be adjusted by the rotating knob. As shown in figure 3, the lens group height, d, is defined as the distance between the bottom of the lens group and the top of object stage. When the lens group locates the lowest displacement, its height is denoted by $d_{\min}$. Similarly, when the lens group locates the highest displacement, $d_{\max}$ denotes the height

of the lens group. While completing the distance from the highest to the lowest, it is assumed that the knob is rotated *n* laps. When the knob is rotated with 1°, the movement of the lens group, Δd, is defined by

$$\Delta d = \frac{d_{\max} - d_{\min}}{n \times 360} \tag{3}$$

When the lens group locates the initial displacement, its height is denoted by d_0, while the angle of the knob is 0°. According to eq. (3), the relationship between the lens group height, d, and the angle of knob, θ, can be established as follows

$$d = d_0 + \theta \times \Delta d \tag{4}$$

In Eq. (4), if the knob is rotated clockwise, $\theta < 0$; otherwise, $\theta \geq 0$.

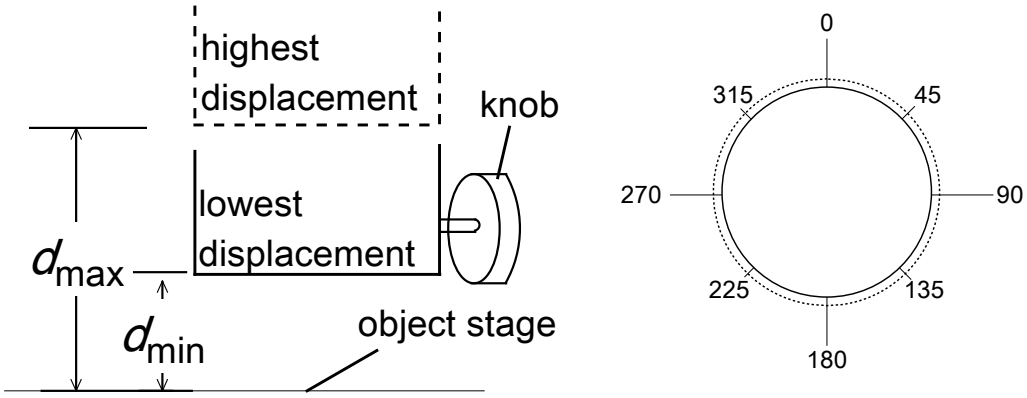

(a) Lens group displacement (b) Knob

Figure 3. Mechanical structure of the object lens

b. Obtaining the relatively sharpest displacement with different zoom rates

In order to compute the relatively sharpest displacement, *T* frames are captured under the condition that the zoom rate is *M*, and the knob is rotated with angle θ from initial 0°. Let $I_{M\theta k}$ represent the *k-th* frame of *T* frames, *k* = 1, 2, …, *T*. Assume that $F_C(\cdot)$ is a definition function, and $F_C(I_{M\theta k})$ is the definition value of the *k-th* frame. As described above, under a specified zoom rate, the sharpest displacement is where $F_C(I_{M\theta k})$ achieves the highest dispacement. Let θ_M denote the sharpest displacement, then, $\theta_M = \arg\max_{\theta}[F_C(I_{M\theta k})]$.

To ensure accuracy, four definition functions are adopted and computed together. If more than three functions indicate that the candidate image is the sharpest, the image will finally be

regarded as the sharpest. The four definition functions used are the image variance function $Q(\bullet)$, the sum of gradient square function $G(\bullet)$, the DFT function $DFT(\bullet)$, and the WHT function $WHT(\bullet)$. They are given by eqs. (5), (7), (8) and (10), respectively.

$$Q(I_{M\theta k}) = \sum_{x=0}^{N-1}\sum_{y=0}^{N-1}[I_{M\theta k}(x,y) - \overline{I_{M\theta k}(x,y)}]^2 \tag{5}$$

where $\overline{I_{M\theta k}(x,y)}$ is the average of $I_{M\theta k}$, given by eq. (6)

$$\overline{I_{M\theta k}(x,y)} = \frac{1}{N^2}\sum_{x=0}^{N-1}\sum_{y=0}^{N-1}(I_{M\theta k}(x,y)) \tag{6}$$

$$G(I_{M\theta k}) = \sum_{x=0}^{N-1}\sum_{y=0}^{N-1}(G_x^2 + G_y^2) \tag{7}$$

In eq. (7), $G_x = I_{M\theta k}(x,y) - I_{M\theta k}(x+1,y)$, $G_y = I_{M\theta k}(x,y) - I_{M\theta k}(x,y+1)$.

$$DFT(I_{M\theta k}) = \sum_{u=0}^{N-1}\sum_{v=0}^{N-1}F_{M\theta k}(u,v) \tag{8}$$

In eq. (8), $F_{M\theta k}(u,v)$ is computed by

$$F_{M\theta k}(u,v) = \sum_{x=0}^{N-1}\sum_{y=0}^{N-1}I_{M\theta k}(x,y)e^{-j2\pi(\frac{ux}{N}+\frac{vy}{N})} \tag{9}$$

where $u = 0,1,\cdots,N-1$, $v = 0,1,\cdots,N-1$.

$$WHT(I_{M\theta k}) = \sum_{u=0}^{N-1}\sum_{v=0}^{N-1}W_{M\theta k}(u,v) \tag{10}$$

In eq. (10), $W_{M\theta k}(u,v)$ is defined as follows:

$$W_{M\theta k}(u,v) = \frac{1}{N^2}\sum_{x=0}^{N-1}\sum_{y=0}^{N-1}W_N(u,x)I_{M\theta k}(x,y)W_N(v,y) \tag{11}$$

where $W_N(n,t)$ is a core function of WHT, and given by

$$W_N(n,t) = \prod_{r=0}^{p-1}(-1)^{n_r n_t} \tag{12}$$

in which $p = \log_2 N$, and n_k is the *k-th* bit of *n* in binary.

c. In-Focus determination model

In order to determine whether or not an image at the relatively sharpest displacement θ_M is in-focus, first, a sharp image of the calibration board under the zoom rate *M* is taken as an original

image for reference.. Let $F_S(I_M)$ denote the definition value of the original image for reference, and $F_C(I_M\theta_M)$ represent the definition value of the relatively sharpest image at θ_M. If the two values are close in proximity, the relatively sharpest image is considered as the in-focus image, and the corresponding displacement is the in-focus displacement. Let *FS* denote the in-focus state, then the in-focus judgment model is described as follows

$$FS = \begin{cases} 1, if \ \dfrac{\left|F_S(I_M) - F_C(I_{M\theta_M})\right|}{F_S(I_M)} < \alpha \\ 0, if \ \dfrac{\left|F_S(I_M) - F_C(I_{M\theta_M})\right|}{F_S(I_M)} \geq \alpha \end{cases} \tag{13}$$

where the factor α, obtained from the experiment, denotes the closed coefficient, which is effected by the zoom rate *M*. If *FS* is equal to 1, it means that the current location is in-focus; otherwise, if *FS* is equal to 0, it means it is out of focus.

d. Fitting the in-focus curve

After completing the above steps, a group of in-focus points, $\{(M^i, \theta_M^i), i = 1,2,\cdots N\}$, will be acquired. Here, *N* is the number of different zoom rates under which the in-focus state *FS* is equal to 1. According to the relationship between the knob angle θ and the lens group height d given in eq. (4), the other group of points $(M^i, d_M^i), i = 1,2,\cdots N$, can be calculated. Finally, an in-focus curve should be fitted according to these results. The curve equation is given as $d = S(M; a_0, a_1, \cdots, a_j)(j < N)$, here, a_l (l = 0, 1, …, j) are the coefficients to be determined, which can be solved according to the computed results $(M^i, d_M^i), i = 1,2,\cdots N$.

To minimize the sum of squared errors, the least-squares method is used to obtain the undetermined coefficients $\{a_l;\ l = 0, 1, \ldots, j\}$. The error between the known pair and the fitted curve is denoted as δ_i (i =1, 2,…,*N*), in which $\delta_i = S(M^i) - d_M^i$. $\sum_{i=1}^{N} \delta_i^2$ should to be minimized.

The target polynomial can be given by

$$S(M; a_0, a_1, \cdots, a_j) = a_0 + a_1 M + a_2 M^2 + \cdots + a_j M^j \tag{14}$$

Then, the sum of squared errors is given by

$$T(a_0, a_1, \cdots, a_j) = \sum_{i=1}^{N} ((a_0 + a_1 M^i + a_2 (M^i)^2 + \cdots + a_j (M^i)^j) - d_M^i)^2 \tag{15}$$

In order to get the minimum value of the target function given by eq. (15), the partial derivative of every undetermined coefficient should be equal to 0. which is shown in eq. (16) below.

$$\frac{\partial T}{\partial a_l} = 2\sum_{i=1}^{N}((a_0 + a_1 M^i + a_2 (M^i)^2 + \cdots + a_j (M^i)^j) - d_M^i)(M^i)^l = 0 \tag{16}$$

where l = 0, 1, …, j. In eq. (16), M^i and d_M^i are known, a_l are variables in the simultaneous equations. According to eq. (16), the undetermined coefficients, a_l, can be determined. Finally, the fitted curve can be obtained through eq. (17).

$$d = S(M) = a_0 + a_1 M + a_2 M^2 + \cdots + a_j M^j \tag{17}$$

Where the independent variable M is the zoom rate, and d is the in-focus displacement.

IV. EXPERIMENTAL RESULTS AND DISCUSSIONS

a. Determining the mechanical parameter of stereo microscope

To evaluate the performances of the proposed method, the NSZ-800 stereo microscope made by NOVEL OPTICS as shown in figure 4(a) is used in the experiments. In figure 4(a), *A* is the knob for adjusting the focus, and *B* is for adjusting the zoom rate. Normally, the zoom rate of a stereo microscope is small, a calibration board with a block size of 0.1*mm* is adopted, and the resolution of the captured image is 1600×1200. Figure 4(b) is an image taken at the zoom rate of 6.5, and the region at the center of the image with the size of 1024×1024 is used to compute the image definition.

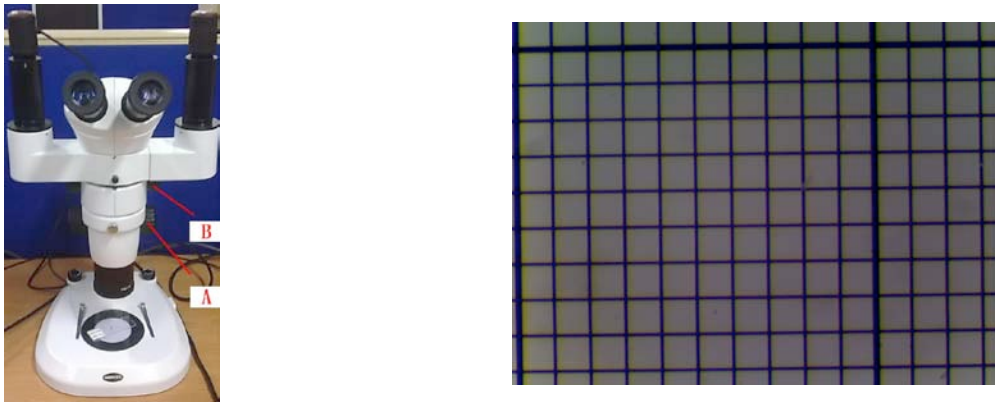

(a) Stereo Microscope (b) Calibration Board

Figure 4. Stereo microscope and calibration board image

Table 2 shows the measurement results of the mechanical parameters described in section 3(a). $d_{\min}$ and $d_{\max}$ are measured three times, and the average of the results is used as the final data. Δd is calculated according to eq. (3).

b. Evaluation of the image definition with different zoom rates

Figure 5(a)-(f) are the definition values with respect to the zoom rates of 6.5, 5, 4, 2, 1 and 0.8, respectively. The four definition functions used are the variance function, the gradient square function, the DFT function, and the WHT function, where the *x-axis* is a rotation angle relative to the base location, and the negative direction is clockwise (CW) while the positive direction is counterclockwise (CCW).

Table 2. Lens group displacement measurement result. *No.* is the measure times, *Measured* is the measuring results in *mm*, *Average* is the average of the values for *Measured* (in *mm*), *TD* is the total knob degree from highest to lowest in *degrees*, Δd is the displacement per degree with unit *mm/degree*.

	No.	**Measured**	**Average**	***TD***	**Δd**
$d_{\min}$	1	34.2	34.2	1690	0.06083
	2	34.0			
	3	34.4			
$d_{\max}$	1	137.0	137.0		
	2	137.2			
	3	136.8			

In figure 5, there appears to be some phenomena concerning definition functions. First, the curve is more precipitous under a high zoom rate than under low zoom rates. As the field depth of the lens group under the high zoom rate is smaller, the same rotation angle under the high zoom rate will affect the image definition, which is more apparent than under the low zoom rate. Thus, the high-precision knob should be used under a high zoom rate. Second, due to the large field depth of the lens group under a small zoom rate, the small rotating angle only affects the image definition a little; thus, a more sensitive definition function should be designed in order to determine the sharpest location quickly. Third, the performance of the gradient square function in eq. (7) is better than that of other definition functions under all the zoom rates. This means that to represent the image definition of the calibration board, the gradient characteristic is more obvious than the other characteristics, such as variance, DFT coefficients and WHT coefficients. Fourth, in figure 5(b), that variance function clearly shows a different result in comparison to the other

three definition functions under the zoom rate 5. Similarly, the DFT function and the WHT function cannot effectively distinguish the definition of images with respect to the focal angles of -1 and 0 under the zoom rate 2. In summary, the gradient square function is more precipitous and robust than the other definition functions in processing the calibration board image obtained from the stereo microscope.

c. In-focus determination

Under the specified zoom rate, first, the knob is manually adjusted to create the sharpest image,

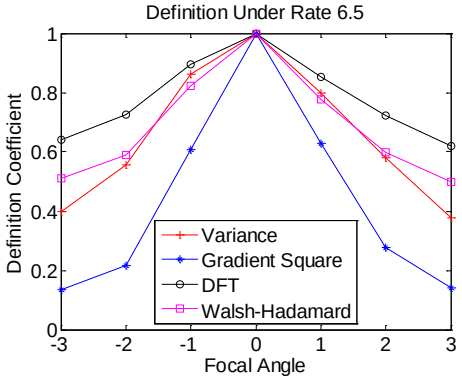

(a) Definition functions with zoom rate of 6.5

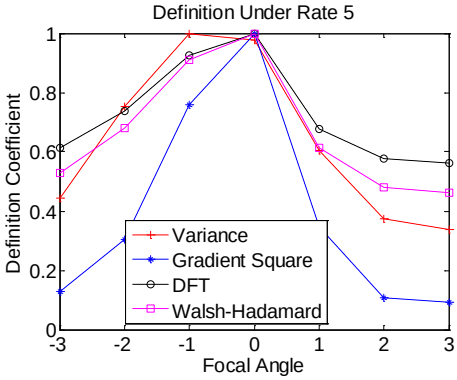

(b) Definition functions with zoom rate of 5

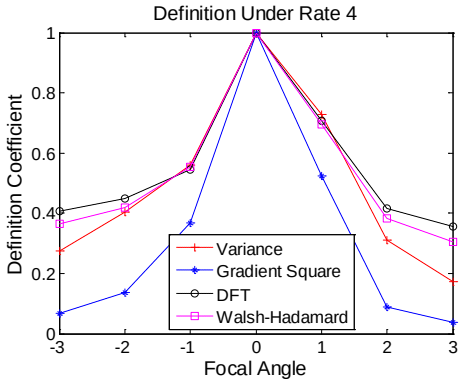

(c) Definition functions with the zoom rate of 4

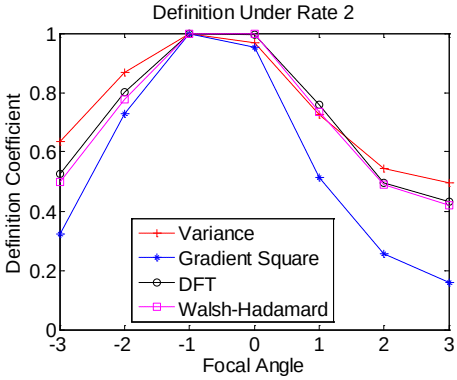

(d) Definition functions with the zoom rate of 2

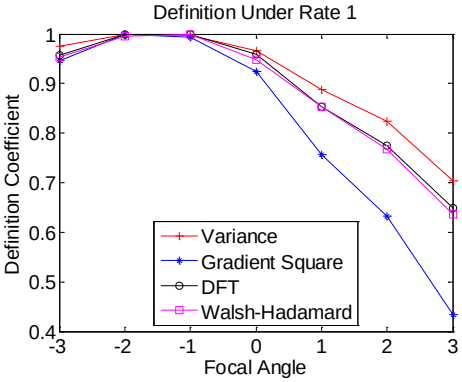

(e) Definition functions with the zoom rate of 1

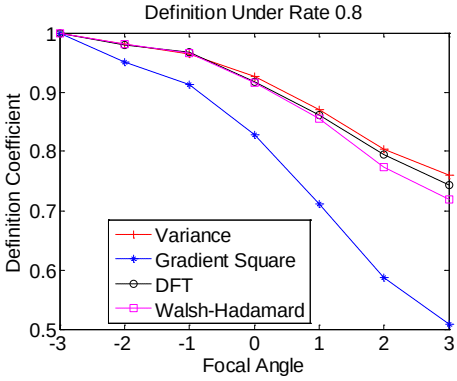

(f) Definition functions with the zoom rate of 0.8

Figure 5. Definition function with different zoom rates

and then 10 photos are taken. Second, the definition function values are calculated. The maximum is denoted by $C_{\max}$ while the minimum is denoted by $C_{\min}$. The equation $(C_{\max} - C_{\min})/C_{\max}$ is used to represent the definition parameter for changing the sharpness of an image in order to make it in focus. Repeating the above steps, a group of definition parameters can be acquired as shown in table 3. Under a different zoom rate, the values of definition drastically change. From the table, the variance function appears the most stable one in the four definition functions except under zoom rate 2, where the DFT function value is the smallest.

Table 3. In-focus definition function value changes under different zoom rates. *M* is the zoom rate, *Q*(.) is the variance function, *G*(.) is the gradient square function, *DFT*(.) is the DFT function and *WHT*(.) is the WHT function.

M	***Q*(.)**	***G*(.)**	***DFT*(.)**	***WHT*(.)**
6.5	0.35%	0.85%	0.48%	0.83%
5	0.61%	1.4%	1.1%	0.99%
4	0.086%	0.44%	0.62%	0.63%
2	1.5%	0.98%	0.43%	1.3%
1	0.058%	0.10%	0.30%	0.27%
0.8	0.15%	0.31%	0.20%	0.23%

As described in section 3(c), the factor α is an important parameter that relates to the zoom rate *M* in the in-focus determination model. Currently, there is not a logical expression to represent α by *M*. In this paper, factor α is obtained through experiments. When adopting the variance function as the definition function, the suggested value of factor α is shown in table 4.

Table 4. Suggesting α with the variance function

	6.5	**5**	**4**	**2**	**1**	**0.8**
α	0.30%	0.56%	0.06%	1.4%	0.038%	0.10%

d. Fitting the continuous zoom parfocality curve

Using the results in subsections 4(b) and 4(c), the in-focus location under a specified zoom rate can be obtained. Without loss of generality, it is assumed that the in-focus location under the rate 6.5 is the initial location, and the corresponding angle of the knob is 0° (as defined in section 3.a where $d_0 = 0$). All in-focus locations are shown in table 5.

During the processing of fitting the curve, third-order, fifth-order and eighth-order polynomials are tried. The results are shown in figure 6. The results from the experiment show that the third-order polynomial is not accurate enough to pass every discrete point from table 5. The amplitude

of swing of the eighth-order polynomial is too large to represent the actual in-focus curve. By contrast, the fifth-order polynomial seems to be optimal.

Table 5. All in-focus locations. IFD is in-focus displacement. Unit of angle is degree, and unit of IFD is *mm*. IFD is calculated according to Eq. (4)

Rate	**6.5**	**5**	**4**	**2**	**1**	**0.8**
Angle	0	1	1	14	55	87
IFD	0	-0.06083	-0.06083	-0.85162	-3.34565	-5.29221

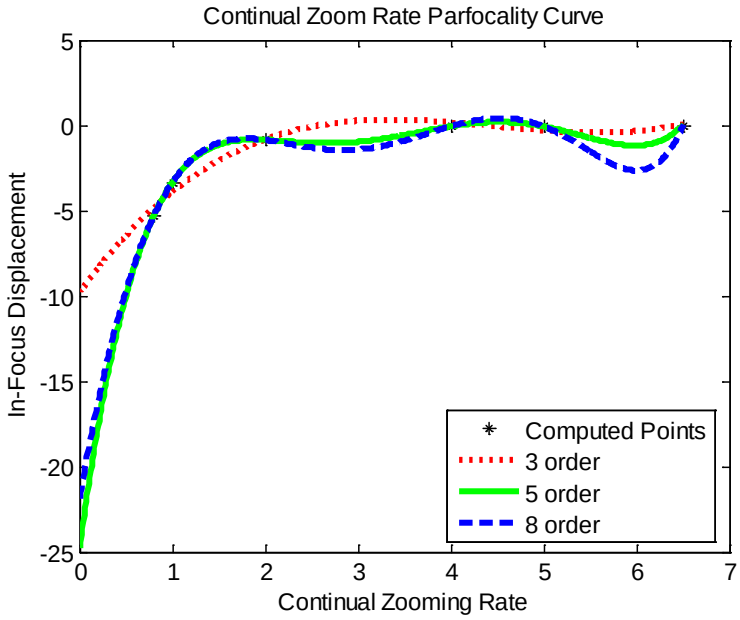

Figure 6. Continuous zoom rate parfocality curve

V. CONCLUSSION

Based on experiments using the in-focus determination model and the definition function, the proposed parfocality measurement method has been proven to be effective and accurate. To fit the features of the calibration board image obtained from the stereo microscope, the four functions, namely, the variance function, the gradient square function, the discrete Fourier transform function and the Walsh-Hadamard transform function, are chosen as definition functions to be used. An image is regarded as the relatively sharpest if there are at least three definition functions finding the candidate as the sharpest. Under the specified zoom rate, the in-focus judgment model, with different factor α from 0.038% to 1.4%, is proposed, and the

parfocality is computed using the proposed model. Finally, according to the computed in-focus image and its corresponding displacement, discrete pairs are obtained to fit the continuous zoom rate parfocality curve. The results from the experiment show that the continuous zoom rate parfocality curve can be measured using the proposed method accurately and effectively.

Based on proposed method and a large number of experiments, the statistical continuous zoom rate parfocality curve can be obtained, which will further improve the quality of the stereo microscope. In the event new data becomes available, a new measurement modal and method will be proposed to increase speed and accuracy of measurements.

Acknowledgments: This work was supported by a grant from the Natural Science Foundation of China (61111140392), and the Ningbo Natural Science Foundation (Grant No.2010A610111, 2011A610200).

REFERENCES

[1] A. S. Murty, K. Aravinda, T. V. Ramanaiah, R. L. V. Petluri, V. V. R. Murthy, and G. R. C. Reddy, "Design of a high-resolution stereo zoom microscope", Optical Engineering, Vol. 36, No. 1, 1997, pp. 201-209.

[2] D. D. Wang, Y. Y. Yang, C. Chen and Y. M. Zhuo, "Calibration of geometrical systematic error in high-precision spherical surface measurement", Optics Communications, Vol. 284, No. Compendex, 2011, pp. 3878-3885.

[3] Z. W. Li and Y. F. Li, "Dense and refined microstructure 3D measurement method based on an optical microscope and varying illuminations", Measurement Science and Technology, Vol. 22, No. 3, 2011, p. 1.

[4] I. Beak, S. Lee and V. Shin, "Robust fusion algorithms for linear dynamic system with uncertainty", International Journal on Smart Sensing and Intelligent Systems, Vol. 3, No. 2, 2010, pp. 146-155.

[5] B. Lechner, M. Lieschnegg, O. Mariani, M. Pircher, and A. Fuchs, "A wavelet-based Bridge Weigh-in-Motion system", International Journal on Smart Sensing and Intelligent Systems, Vol. 3, No. 4, 2010, pp. 573-591.

[6] H. Yamamoto and T. Sano, "Study of micromanipulation using stereoscopic microscope", IEEE Transactions on Instrumentation and Measurement, Vol. 51, No. 2, 2002, pp. 182-187.

[7] M. Jahnisch and M. Schiffner, "Stereoscopic depth-detection for handling and manipulation tasks in a scanning electron microscope", IEEE International Conference on Robotics and Automation, Orlando, USA, 2006, pp. 908-913.

[8] J. Bert, S. Dembele and N. Lefort-Piat, "Performing Weak Calibration at the Microscale, Application to Micromanipulation", IEEE International Conference on Robotics and Automation, Roma, Italy, 2007, pp. 4937-4942.

[9] Q. Lu, Y. Ji and W. Shen, "Design of a fore continual zoom system with high speed", Acta Optica Sinica, Vol. 30, No. 9, 2010, pp. 2674-2679.

[10] A. R. Backes, A. S. Martinez and O. M. Bruno, "Texture analysis using graphs generated by deterministic partially self-avoiding walks", IEEE Transactions on Pattern Recognition, Vol. 44, No. 8, 2011, pp. 1684-1689.

[11] Y. Al-Kofahi, W. Lassoued, W. Lee and B. Roysam, "Improved Automatic Detection and Segmentation of Cell Nuclei in Histopathology Images", IEEE Transactions on Biomedical Engineering, Vol. 57, No. 4, 2010, pp. 841-852.

[12] A. Sengur and Y. Guo, "Color texture image segmentation based on neutrosophic set and wavelet transformation", Computer Vision and Image Understanding, Vol. 115, No. 8, 2011, pp. 1134-1144.

[13] M. Baro and J. Ilow, "Space-Time Block Codes Based on Diagonalized Walsh-Hadamard Transform with Simple Decoupling", Vehicular Technology Conference Fall (VTC 2010-Fall), Ottawa, Canada, 2010, pp. 1-5.

[14] J. Jaehwan, L. Jinhee and P. Joonki, "Robust focus measure for unsupervised auto-focusing based on optimum discrete cosine transform coefficients", IEEE Transactions on Consumer Electronics, Vol. 57, No. 1, 2011, pp. 1-5.

[15] S. Yousefi, M. Rahman, N. Kehtarnavaz and M. Gamadia, "A new auto-focus sharpness function for digital and smart-phone cameras", IEEE International Conference on Consumer Electronics, Las Vegas, USA, 2011, pp. 475-476.

[16] J. W. Han, J. H. Kim, H. T. Lee and S. J. Ko, "A Novel Training Based Auto-Focus for Mobile-Phone Cameras", IEEE Transactions on Consumer Electronics, Vol. 57, No. 1, 2011, pp. 232-238.

[17] S. A. Eastwood, D. M. Paganin and A. C. Y. Liu, "Automated phase retrieval of a single-material object using a single out-of-focus image", Optics Letters, Vol. 36, No. 10, 2011, pp. 1878-1880.

[18] X. T. Li and Z. F. Cen, "Geometrical Optics, Aberrations and Optical Design". Hangzhou: Zhejiang University Press, 2007.